

**EMPIRICAL MODELS FOR ESTIMATING
PRECIPITABLE WATER USING ADVANCED
TIROS OPERATIONAL VERTICAL SOUNDER
SATELLITE DATA OVER PENINSULAR
MALAYSIA**

MAKAMA EZEKIEL KAURA

UNIVERSITI SAINS MALAYSIA

2018

**EMPIRICAL MODELS FOR ESTIMATING
PRECIPITABLE WATER USING ADVANCED
TIROS OPERATIONAL VERTICAL SOUNDER
SATELLITE DATA OVER PENINSULAR
MALAYSIA**

by

MAKAMA EZEKIEL KAURA

**Thesis submitted in fulfillment of the requirements
for the degree of
Doctor of Philosophy**

September 2018

DEDICATION

To my beloved wife, Asabe; my adorable children, Rhishama and Rhituomoh; my parents, Azumi and Kaura Zaki of blessed memories.

CERTIFICATION

This thesis entitled ‘Empirical Models for Estimating Precipitable Water using Advanced TIROS Operational Vertical Sounder Satellite Data over Peninsular Malaysia’ was carried out by Makama Ezekiel Kaura under the supervision of Associate Professor Dr. Lim Hwee San and Professor Dr. Khirrudin Bin Abdullah, School of Physics, Universiti Sains Malaysia. Haven satisfy the requirements for the degree of Doctor of Philosophy (Atmospheric Sciences) of the Universiti Sains Malaysia it is hereby approved, after due examination and defence, for its contribution to scientific knowledge and literally input.

.....
Assoc. Prof. Dr. Lim Hwee San
Main Supervisor

.....
Date

.....
Prof. Dr. Khiruddin Bin Abdullah
Co-Supervisor

.....
Date

.....
Prof. Dr. Azlan Abdul Aziz
Dean, School of Physics

.....
Date

.....
Prof. Dr. Rozman Bin Hj Din
Dean, Institute of Post Graduate Studies

.....
Date

ACKNOWLEDGEMENT

I am profoundly grateful to God All Mighty, whose grace and mercies sustained and nurtured me every inch of my sojourn at Universiti Sains Malaysia. His enduring love and mercy kept me in good health during this research. May His name be forever, praised.

With deep sense of gratitude, I acknowledge the untiring efforts and counsel of my main supervisor, Associate Professor Dr. Lim Hwee San, who, despite his busy schedule, created time and space to ensure that this dissertation was successfully completed. I am indebted to Professor Khiruddin Bin Abdullah, who co-supervised this work, for placing his wealth of experience at my disposal. His critical observations and invaluable suggestions added flare to the research. I appreciate members of staff in the School of Physics, Universiti Sains Malaysia, who facilitated this research one way or another. My informal discussion at different times with Drs. Ismail Bin Ahmad Abir and Fuyi Tan provided useful information.

I am grateful to the Vice Chancellor and Management of the University of Jos, Nigeria, for the opportunity and support offered me to undertake this research work. I also appreciate the head, Department of Physics, University of Jos and other colleagues for their prayers and goodwill during this study.

I am deeply grateful to my siblings, Messrs. Mark and Jacob Kaura, for their prayers and financial support. I also note the moral support received from Atanda and James Kaura. Etched in my memories is the brotherly love accorded me by friends and associates from USM and EPCC, whose names are too numerous to mention here for want of space. Of note, however, are Drs. M. J. Marut, G. G. Zaku,

V. Davidson, P. N. Dashe, D. O. Ojatta, P. Wash, and Bro Choo. Thank you for your selfless sacrifices to make my stay in Malaysia a memorable experience.

The satellite, meteorological, and radiosonde data used in this work were respectively provided by the Satellite Application Facilities on Climate Monitoring (CM-SAF) at Deutscher Wetterdienst in Germany, NOAA's National Center for Environmental Information (NCEI), and the University of Wyoming sounding archives, to whom I offer my gratitude.

Finally, I deeply appreciate the tremendous support from my loving and kind-hearted wife, Asabe, who held in trust, all of my responsibilities, handling every challenge with utmost commitment throughout the duration of this study. May the Lord bless and keep you. To my children, Pat, Rhisha, and Rhituo, I say thank you for your patience and the wonderful support you gave your mother while she handled the home front in my absence.

TABLE OF CONTENTS

ACKNOWLEDGEMENT	ii
TABLE OF CONTENTS	iv
LIST OF TABLES	ix
LIST OF FIGURES	xii
LIST OF SYMBOLS	xvii
LIST OF ABBREVIATIONS	xix
ABSTRAK	xxiv
ABSTRACT	xxvi
CHAPTER 1 - INTRODUCTION	1
1.1 Background of the Study.....	1
1.1.1 The Structure of the atmosphere	8
1.1.2 Gaseous composition of the Atmosphere.....	9
1.1.3 Pressure and temperature profiles of the Atmosphere	10
1.1.4 The Troposphere	10
1.2 Probing the Earth's atmosphere from space.....	11
1.3 Statement of the Research Problem	12
1.4 Aim and Objectives.....	14
1.5 Research Question.....	15
1.6 Research Hypothesis	15
1.7 Scope of the Study	16
1.8 Novelty and Significance of the Study.....	17
1.9 Thesis Outline	18

CHAPTER 2 – LITERATURE REVIEW	21
2.1 Introduction	21
2.2 Importance of Precipitable Water Study	21
2.2.1 The hydrologic cycle.....	22
2.2.2 The effects of precipitable water on radiation balance	23
2.2.3 Predictions of clouds and precipitation.....	25
2.3 A Brief Description of Global and Regional Wind Patterns.....	26
2.3.1 Global.....	27
2.3.2 Regional	29
2.4 Some Local Impacts of Precipitable Water in Peninsular Malaysia	30
2.5 Global and Regional Observations of Precipitable Water	31
2.5.1 In situ-based observation methods.....	33
2.5.2 Satellite remote sensing	35
2.5.3 Empirical model /simulation methods	40
2.5.4 Artificial neural networks	46
2.6 Comparison between Radiosonde and Satellite Precipitable Water	50
2.7 Total Precipitable Water Climatology	53
2.7.1 Spatial and temporal variabilities of precipitable water.....	53
2.7.2 Inter- layer formulation of tropospheric water vapour.....	60
2.8 Summary	61
 CHAPTER 3 – METHODOLOGY	 62
3.1 Introduction	62
3.2 Study Area.....	62
3.3 Climate of Peninsular Malaysia	64

3.4	Description of Datasets and their Sources	65
3.4.1	Mean wind vector maps	65
3.4.2	Mean sea level pressure.	66
3.4.3	Surface meteorological data.....	66
3.4.4	Radiosonde data	69
3.4.5	ATOVS data.....	70
3.5	Software and Tools	75
3.6	Data Analysis	76
3.6.1	Generation of seasonal air flow pattern (vector wind maps)	78
3.6.2	Mean sea level pressure	78
3.6.3	Analysis of surface meteorological data	78
3.6.4	Derivation of TPW from radiosonde data.....	79
3.6.5	Analysis of ATOVS data	82
3.7	Models and Performance Evaluation	85
3.7.1	Empirical models using multiple linear regression method.....	86
3.7.2	Models performance evaluation.....	92
3.7.3	Artificial neural network models	93
3.8	Summary of the Procedures	97
CHAPTER 4 – RESULTS AND DISCUSSION.....		101
4.1	Introduction	101
4.2	Climatology of Precipitable water data from ATOVS.....	101
4.2.1	Zonal demarcation of the study area.	102
4.2.2	Variation of total precipitable water	103
4.2.3	Temporal variation of layered precipitable water	106

4.2.4	Comparison between radiosonde- and ATOVS-derived data.....	110
4.3	Relationships between Layers of Precipitable Water.....	119
4.3.1	Spatial distribution of total precipitable water.....	120
4.3.2	Spatial distribution of layered precipitable water	122
4.3.3	Inter-layer correlation and model development.....	124
4.3.4	Validation of Inter-layer models.....	132
4.3.5	Comparison with previously reported models	135
4.4	Variability of Surface Meteorological Parameters.....	138
4.4.1	Seasonal wind flow patterns and sea level pressure	138
4.4.2	Temporal and spatial variations of temperature.....	140
4.4.3	Temporal and spatial distribution of relative humidity.....	144
4.5	Development of models to Estimate TPW using MLR method	149
4.5.1	Statistical criteria for model selection.....	149
4.5.2	Evaluation of model diagnostics.....	151
4.5.3	MLR accuracy test and influence of surface parameters on TPW...	154
4.5.3	Model Validation	164
4.5.4	Comparison between the proposed models and other models	167
4.5.5	Evaluation of Artificial Neural Network	170
4.5.6	Comparison between MLR and ANN models.....	174
4.6	Summary	176
	CHAPTER 5 – CONCLUSION AND RECOMMENDATION.....	177
5.1	Conclusions	177
5.2	Recommendations for Further Work	179

REFERENCES..... 181

APPENDIX

LIST OF PUBLICATIONS

LIST OF TABLES

		Page
Table 1.1	Number of radiosonde stations from which reports are received at ECMWF for 2016 by World Meteorological Organization (WMO) region. For 0000 UTC and 1200 UTC. These are those that report 30 hPa temperature at least 25 times	6
Table 1.2	Gaseous composition of the atmosphere (Source: http://geogrify-.net/GEO1/Images/FOPG/03T2)	10
Table 3.1	Delineated geographic zones in the study area	70
Table 3.2	Satellite combinations and corresponding period used to generate the ATOVS humidity and temperature profiles for the retroactively produced Climate Data Records (CDRs)	70
Table 3.3	Water vapour channels, frequencies and maximum sensitivity pressure levels for the sounding sensors onboard NOAA-15 to -19 and Metop-A satellites	72
Table 3.4	Location of the geographic zones and radiosonde stations in the study area	77
Table 3.5	Layers of precipitable water with corresponding elevation and pressure levels for radiosonde observations	81
Table 3.6	Levels of precipitable water (S5 – S1) and how they were combined to obtain the different layers used in this work. The pressure range for each level is indicated	84
Table 4.1	Monthly and annual mean TPW (mm) for the period 2001 – 2011 across the three zones	105
Table 4.2	Regression of TPW and WRT at all the isobaric levels, showing values of best-fit parameters, α and β (i.e. $TPW = \beta \cdot WRT + \alpha$). MBE and RMSE are in mm. The probability value at 0.05 significance are also shown	112

Table 4.3	Regression of TPW and WRT at all the isobaric layers, showing values of best-fit parameters, α and β (i.e. $TPW = \beta \cdot WRT + \alpha$) for the NEM and SWM. The coefficient of determination (R^2), probability values (p) at 0.05 significance, with remark are also shown. ‘S’ – significant and ‘NS’ – not significant	118
Table 4.4	Best Fit regression constants (α , β), correlation coefficient, r, and the probability, p, in the regression of lower layer precipitable water (WL) on the Middle (WM) and upper (WH) layers precipitable water, using CDR (2001 – 2011) data for the 3 zones and the entire study area. N is the number of observations and CV is the coefficient of variation	127
Table 4.5	Mean values of the predicted middle (WM) and upper (WH) layers PW using Equation (4.5a and b) on the training data (CDR 2001 – 2011). The observed values, mean bias (MBE), and root mean square errors (RMSE) for both layers across the 3 zones are also shown. All values are in mm	132
Table 4.6	The coefficient of determination (R^2), mean bias (MBE), and root mean square (RMSE) values obtained, using Equation (4.5a, b) on the testing data OP (2012 – 2015), across the 3 zones. Both MBE and RMSE are in mm	135
Table 4.7	Previous models for the estimation of middle and upper layers PW and their statistical parameters (mean monthly PW, MB and RMSE) are compared with the observed mean monthly values ($WM = 25.90$, $WH = 30.05$) at the northern zone of Peninsular Malaysia for the period 2005 – 2011. The MBE, RMSE were respectively 0.17, 1.65 for Equation 4.5a and 0.34, 1.96 for Equation 4.5b. All the quantities are in mm unit	137
Table 4.8	Monthly-mean values of the surface meteorological data used in the three zones for the period 2001 – 2011	141
Table 4.9	All possible models involving the three meteorological parameters for the estimation of total precipitable water (TPW) in the study area	150
Table 4.10	Regression coefficients for the seasonal and overall model obtained in the northern (NZ), central (CZ), and southern (SZ) zones using monthly mean ATOVS data for the period 2001 – 2011. Significance of the relationship, and number of observations are also given	150
Table 4.11	Statistical test on all model subsets for the prediction of TPW using the overall data (Jan – Dec) in the 3 zones, showing mean bias error (MBE/mm), root mean squared errors (RMSE/mm), and coefficient of determination (R^2)	152

Table 4.12	Performance evaluation of the developed seasonal and overall models for the three regions using mean bias (MBE), root mean squared error (RMSE) and coefficient of determination (R ²). Both MBE and RMSE are in mm	157
Table 4.13	Standardized regression coefficients (β) for the monthly models at the three zones, using ATOVS data for 2001 – 2011. Variables that are not significant at the 95% confident level for each month are ast	162
Table 4.14	Mean values of the observed and predicted TPW using Equation (4.6 – 4.8) on the independent datasets: OP (2012 – 2015) and surface (2012 – 2015). The observed values, mean bias (MBE), and root mean square errors (RMSE) across the 3 zones are also shown. All values, except for R ² , are in mm	165
Table 4.15	Comparison between selected empirical models and those proposed for the overall period in this study	169
Table 4.16	Performance evaluation of the neural network models using Levenberg-Marquardt (LM) and Bayesian Regularization (BR) training algorithm in feedforward network. The RMSE values for the training sessions are also given for each period	172

LIST OF FIGURES

		Page
Figure 1.1	Phase transitions of water in the hydrologic cycle	1
Figure 1.2	Global monthly total precipitable water vapour (TPW) for 2009 derived from Advanced TIROS Operational Vertical Sounder (ATOVS) measurements (Courcoux & Schröder, 2015)	2
Figure 1.3	Annual mean specific humidity (Oort, 1983). The red solid line indicates humidity variation for the latitude 100 S – 100 N, the green and blue dash-lines are for latitudes 400 – 500 N and 700 – 800 N respectively	3
Figure 1.4	Global radiosonde network (Courtesy: NOAA’s National Weather Service)	5
Figure 1.5	Global distribution of integrated surface database (source: NCEI-NOAA)	6
Figure 1.6	The Structure of the Atmosphere, showing the variation of global temperature with altitude and pressure (Source: Teachertech, 2006)	9
Figure 2.1	Long-term mean estimates of global water budget and its annual flow based on Trenberth, et al. (2007). Estimates are in 103 km ³ for storage and 103 km ³ /year for exchanges	23
Figure 2.2	Global wind patterns: Thick red arrows are Trade-winds (warm tropical air masses), thick green arrows are Westerlies (cold air masses in the mid- and higher- latitudes), and light blue are Easterlies. Red and green thin arrows represent warm and cold air respectively. (Redrawn from Global Wind Images)	28
Figure 2.3	(a) annual mean total precipitable water from NVAP data for the period 1988-1992. (b) profile of zonal mean TPW in millimetres. Source: Trenberth (1998)	54
Figure 2.4	Zonal mean monthly TPW (mm) for July 2004 for NOAA (dashed line) and Aqua AMSR (solid line). Source: Ferraro et al. (2005)	55

Figure 2.5	Mean diurnal TPW anomaly on (a) high solar radiation and (b) low solar radiation days. [Source: Wu et al. (2003)]	59
Figure 3.1	The Map of Peninsular Malaysia, depicting the location of meteorological stations used in the study with centre-dotted circles. Blue, green, and red circles represent stations in the northern, central and southern zones respectively	63
Figure 3.2	Schematic flowchart for the comparison of ATOVS precipitable water with that derived from radiosonde observations to establish data climatology in Peninsular Malaysia	82
Figure 3.3	Work flow for temporal and spatial analysis of TPW and meteorological parameters	85
Figure 3.4	Workflow for the formulation of inter-layer relationship	88
Figure 3.5	Criteria for model development using MLR method	92
Figure 3.6	The schematic architecture of the ANN implemented for the estimation of precipitable water vapour	97
Figure 3.7	Schematic summary of the methodology adopted to achieve the main objectives of the current study	100
Figure 4.1	The demarcation of the Study Area based on the spatial variational patterns of the lower layer precipitable water (WL) with latitude (ϕ). SZ, CZ, and NZ represent southern, central, and northern zones respectively	102
Figure 4.2	Monthly variation of total precipitable water vapor (TPW) for 2001 – 2011 over the climatic regions of Peninsular Malaysia as retrieved from the CM SAF-ATOVS water vapor product	104
Figure 4.3	Mean monthly distribution of TPW in millimeters (mm) for 2001 – 2011 period	106
Figure 4.4	Monthly mean distribution of layered precipitable water vapour (TPW) ATOVS (2001 – 2011): (a) NZ, (b) CZ, and (c) SZ of Peninsular Malaysia	109
Figure 4.5	Comparison between ATOVS and radiosonde data for Penang, Kuantan, and Sepang stations as representatives of the northern, central, and southern zones respectively. WRL, WRM, and WRU are lower, middle and upper layer PW for radiosonde, while WSL, WSM and WSU are for ATOVS	111

Figure 4.6	Mean bias (MBE) between the satellite (ATOVS) and radiosonde monthly mean layered precipitable water for the radiosonde stations of (a) Penang (b) Kuantan, and (c) Sepang	113
Figure 4.7	Scatter-plots and least square regression lines of the absolute difference in PW ($WD = TPW - WRT$) against TPW at the different layers and for the three stations that had radiosonde data	116
Figure 4.8	Seasonal mean TPW (2001 – 2011) over Peninsular Malaysia. (a) NEM (b) SWM. Contours are shown in mm	121
Figure 4.9	Precipitable water for the lower layer (upper panel), middle layer (middle panel), and upper layer (lower panel) during the NEM and SWM seasons over Peninsular Malaysia using CDR (2001 – 2011)	124
Figure 4.10	Mean annual middle (WM) and upper (WH) precipitable water vapour as functions of latitude (ϕ), for the period 2001–2011. Error bars are standard deviations of each monthly averages from mean annual values. The linear fit equations between ϕ and annual mean WM/WH are given. The applicability of each equation is given by the values of R ²	129
Figure 4.11	Scatter-plots of: (a) lnWL against lnWM. (b) lnWL against lnWH, for all the zones. (c) The regression lines of lnWL against lnWM and lnWH, with the best-fit regression equations for the entire Peninsular Malaysia	130
Figure 4.12	Comparisons between the observed and predicted LPW for the entire study area using the original data (CDR: 2001 – 2011). Top panel is for northern zone; Middle panel is for central zone; bottom is for southern zone. The solid lines are the regression fits between the observed and predicted values of WM and WH. The dashed are the 1:1 reference lines	133
Figure 4.13	Mean wind speed (m/s) and directions for the period of 2001 – 2011 over Peninsular Malaysia. (a) Northeast monsoon (NEM). (b) Southwest monsoon (SWM)	139
Figure 4.14	Mean sea level pressure (hPa) for the period 2001 – 2011 over Peninsular Malaysia. (a) Northeast monsoon (NEM). (b) Southwest monsoon (SWM)	140
Figure 4.15	Annual cycle of temperature in the three zones of Peninsular Malaysia. Red, black and green lines are for northern, central and southern zones respectively	142
Figure 4.16	Seasonal distribution of temperature (T) in Peninsular Malaysia, using surface data for the period 2001 – 2011	144

Figure 4.17	Annual cycle of relative Humidity in the three zones of Peninsular Malaysia. Red, black and green lines are for northern, central and southern zones respectively	145
Figure 4.18	Seasonal distribution of relative humidity (H) in Peninsular Malaysia, using surface data for the period 2001 – 2011	148
Figure 4.19	Normal probability and P-P plots of the residuals obtained using the overall ATOVS CDR data for the period 2001 – 2011. Top row – northern zone, middle row – central zone, and last row – southern zone	154
Figure 4.20	Mean monthly coefficient of determination (R^2), (b) mean monthly root mean square error (RMSE), (c) monthly mean bias error (MBE) for model calibration in northern (NZ), central (CZ), and southern (SZ) zones using CDR (2001 – 2011) data	156
Figure 4.21	Comparisons between the observed and predicted TPW for northern (NZ), central (CZ), and southern (SZ) zones, using the overall ATOVS CDR (2001 – 2011) data. The solid lines are the regression fits between the observed and predicted values of TPW. The dashed are the reference lines	160
Figure 4.22	Seasonal plots of actual total precipitable water against predicted values from the three zones in Peninsular Malaysia using ATOVS CDR (2001 -2011) data. The left column is for northeast monsoon (NEM) while right column is for southwest monsoon (SWM) periods. NZ, CZ, and SZ represent northern, central, and southern zone, in that order	161
Figure 4.23	Scatter plots of observed against predicted TPW for the overall season, using Equation (4.6 – 4.8) on the independent datasets: OP (2012 – 2015) and surface (2012 – 2015): (a) north zone (b) central (c) south. R^2 values are also included	165
Figure 4.24	Comparison between observed TPW from OP (2012 – 2015) data and predicted TPW obtained using the seasonal models. The top, middle, and bottom rows are for the north (NZ), central (CZ), and south (SZ) respectively. The left column depicts northeast monsoon (NEM) season, while the right is for the southwest monsoon (SWM). Corresponding values of R^2 are also shown	167
Figure 4.25	Comparisons between the measured TPW and predicted TPW using feed forward network in Levenberg-Marquadt (LM) and Bayesian Regularization (BR) training algorithms for the ATOVS-CDR (2001 – 2011). (a) northern zone, (b) central zone, and (c) southern zone. The dashed line is a 1:1 reference line	173

- Figure 4.26 Comparison of the MLR and ANN models using overall season. The statistical parameters of RMSE (mm) and R² values in the north, central and south zones are shown 174
- Figure 4.27 Plots of observed TPW from CDR (2001 – 2011) and predicted TPW using MLR and ANN (LM & BR) against Months of year for the overall season. (a) northern zone (b) central zone (c) southern zone 175

LIST OF SYMBOLS

Ar	Argon
CO_2	Carbon dioxide
R^2	Coefficient of determination
R_S^2	Coefficient of determination for ANN testing
R_T^2	Coefficient of determination for ANN training
r	Correlation coefficient/Mixing ratio
$^{\circ}C$	Degree Celsius
$^{\circ}F$	Degree Fahrenheit
T_d	Dew point temperature
WD	Difference between radiosonde and satellite precipitable water
φ	Latitude
CH_4	Methane
N_2	Nitrogen
N_2O	Nitrous oxide
O_2	Oxygen
O_3	Ozone
P	Pressure
$\alpha_{0.05}$	Probability value at 95% confidence interval
W_R	Radiosonde precipitable water
α	Regression constant
H	Relative humidity
W_S	Satellite precipitable water

e_s	Saturated water vapour pressure
q	Specific humidity
β	Standardized regression coefficient
T_d	Temperature
B	Unstandardized regression coefficient
σ^2	Variance
H_2O	Water vapour
w_p	Water vapour content
e_0	Water vapour pressure
X_2	Xenon

LIST OF ABBREVIATIONS

AGU	American Geophysical Union
AIRS	Atmospheric Infrared Sounder
AMFIS	Adaptive Neuro Fuzzy Interference
AMSR-E	Advanced Microwave Scanning Radiometer-Earth observation system
AMSU-A	Advanced Microwave Sounder Unit - A
AMSU-B	Advanced Microwave Sounder Unit - B
ANOVA	Analysis of Variance
ArcGIS	Aeronautical Reconnaissance Coverage Geographic information system
ASCII	America Standard Code for Information Interchange
ATOVS	Advanced TOVS
BDAC	British Atmospheric Data Centre
CDA	Command and Data Acquisition
CDR	Climate Data Records
CM-SAF	Satellite Applications Facility for Climate Monitoring
CORS	Continuous Operating Reference Station
cT	Continental tropical air mass
CZ	Central Zone
ECMWF	European Centre for Medium-Range Weather Forecast
ECV	Essential Climate variables
ENSO	EL-Nino Southern Oscillation
EUMETSAT	European Organization for the Exploitation of Meteorological Satellites
FCDRs	Fundamental Climate Data Records

FIM	First Inter-monsoon
FORTRAN	Formula Translation
GCOS	Global Climate Observing System
GLOBE	Global Learning and Observations to Benefit the Environment
GNSS	Global Navigation Satellite System
GOES	Global Observational Environmental Satellites
GOME	Global Ozone Monitoring Experiment
GPS	Global Positioning System
GUAN	GCOS Upper-Air Network
HIRS	High Resolution Radiation Sounder
HOMR	Historical Observation Meta Data Repository
IAPP	International ATOVS Processing Package
ICDRs	Interim Climate Data Records
IGRA	Integrated Global Radiosonde Archives
IOD	Indian Ocean Dipole
IPCC	Intergovernmental Panel on Climate Change
IR	Infrared radiation
ITCZ	Inter-Tropical Convergent Zone
ITD	Inter Tropical Discontinuity
KARL	Koldewey Aerosol Raman Lidar
LASER	Light Amplification by Stimulated Emission of Radiation
LIDAR	Light detection and ranging
LPW	Layered precipitable water
MATLAB	Matrix Laboratory
MBE	Mean bias error

Metop	Meteorological Operational Satellite
MHS	Microwave Humidity Sounder
MLP	Multilayer Perceptron
MLR	Multiple linear regression
MODIS	Moderate Resolution Imaging Spectrometer
mT	Tropical maritime air mass
MyRTKnet	Malaysian Real-time Kinetic GNSS Networks
NAO	North Atlantic Oscillation
NASA	National Aeronautics and Space Administration
NCAR	National Centre for Atmospheric Research
NCDC	National Climate Data Center
NCEI	National Centre for Environmental Information
NCEP	Centre for Environmental Prediction
NEM	Northeast Monsoon
NetCDF	Network Command Data File
NGDC	National Geophysical Data Center
ANN	Artificial neural networks
NOAA	National Oceanic and Atmospheric Administration
NVAP	NASA Water Vapour Project
NVAP-NG	NASA Water Vapour Project - Next Generation
NWP	Numerical Weather Prediction
NZ	Northern Zone
Obs	Observed
OP	Operational data
PDO	Pacific Decadal Oscillation

Pre.	Predicted
PW	Precipitable water
RMSE	Root mean squared error
SCIAMACHY	Scanning Imaging Absorption SpectroMeter for Atmospheric CHartography
SIM	Second Inter-monsoon
SLP	Sea level pressure
SPCZ	South Pacific Convergent Zone
SPSS	Statistics Package for the Social Sciences
SSM/I	Special Sensor Microwave/ Imager
SWM	Southwest monsoon
SZ	Southern Zone
TCDRs	Thematic Climate Data Records
TIROS-N	Television and Infrared Observation Satellites
TOVS	Television and Infrared Observation Satellite Operational Vertical Sounder
TPW	Total precipitable water
UTC	Universal Time Coordinate
UTH	Upper Tropospheric Humidity
VIF	Variance Inflation Factor
WH	Upper layer precipitable water
WL	Lower layer precipitable water
WM	Middle layer precipitable water
WMO	World Meteorological Organization
WRL	Lower layer precipitable water(radiosonde)
WRM	Middle layer precipitable water (radiosonde)

WRT	Total precipitable water (radiosonde)
WRU	Upper layer precipitable water (radiosonde)
WU	Upper layer precipitable water
WVR	Water Vapour Radiometer

**MODEL EMPIRIK UNTUK MENGANGGARKAN AIR BOLEH KERPAS
DENGAN MENGGUNAKAN DATA SATELIT ADVANCED TIROS
OPERATIONAL VERTICAL SOUNDER DI SEMENANJUNG MALAYSIA**

ABSTRAK

Air boleh kerpas (PW) merupakan satu pemboleh ubah yang giat berubah, tetapi gas rumah hijau ini penting untuk mengawal bajet sinaran bumi. Pengetahuan yang mencukupi mengenai pengagihan dari segi ruang dan masa adalah diperlukan untuk penerangan dan pemahaman yang lebih baik mengenai cuaca dan iklim global. Terdapat beberapa kajian di Semenanjung Malaysia yang mengangkar jumlah air yang kerpas (TPW) dengan menggunakan data in situ, cara ini kurang mempertimbangkan situasi persekitaran dengan mengeluarkan kesan peredatan tempatan dan perbezaan topografi yang dianggap penting dalam kajian cuaca berskala kecil. Penggunaan parameter meteorologi tunggal untuk menganggarkan TPW biasanya melemahkan parameter lain yang mungkin mempunyai kesan gabungan pada wap air lajur. Oleh sebab ini, algoritma baru berdasarkan regresi linear berganda (MLR) untuk menganggarkan TPW dicadangkan dengan menggunakan rekod data iklim homogenisasi yang diperolehi dari ATOVS di atas NOAA bersama dengan pemerhatian permukaan untuk tempoh 2001 - 2011. Data ATOVS mempunyai padanad yang baik dengan pengukuran radiosonde dari segi spasial mahupun musim dengan pekali korelasi (r) dari 0.60 - 0.98. Hubungan baru antara lapisan bawah (WL) dan lapisan lain yang lebih tinggi, daripada bentuk $W = \alpha(\varphi)[WL]^{\beta(\varphi)}$ telah dicadangkan, dengan W adalah lapisan tengah atau lebih tinggi PW, β ialah koefisien yang berfungsi latitud (φ). Model-model ini memberikan kesilapan persegi dan rintangan akar min (RMSE) dari nilai masing-masing antara

0.867 - 0.926 dan 1.65 - 2.38 mm bagi kedua-dua ramalan WM dan WH di zon yang digariskan. Gambaran keseluruhan pengedaran spatial TPW purata bermusim menunjukkan penurunan secara umum dari selatan ke utara di Semenanjung Malaysia, dengan gradien mendatar di sepanjang sempadan barat semasa NEM. Kadar variasi bulanan bagi spatial dan temporal pada parameter meteorologi yang terpilih menunjukkan bahawa kitaran tahunan dan corak spatial kelembapan relatif padan dengan TPW, dengan nilai maksimum diperolehi dalam SWM dan sekurang-kurangnya semasa tempoh NEM. Nilai yang lebih tinggi didapati secara spatikal dalam SZ dengan nilai yang lebih rendah yang digambarkan di NZ. Suhu menunjukkan struktur yang hampir seragam di zon dengan nilai maksimum pada bulan Mei / Jun dan nilai yang berkurangan pada bulan Januari. Secara umumnya kelembapan relatif mempunyai kesan spatial dan temporal yang dominan pada TPW di seluruh kawasan kajian. Algoritma baru yang dicadangkan untuk menganggarkan TPW memberikan hasil yang sangat menggalakkan dalam semua zon. Bagi tempoh gabungan, nilai R^2 adalah 0.967, 0.946, dan 0.935 di NZ, SZ, dan CZ masing-masing, dengan nilai MBE dan RMSE pada 0.09, 0.81, -0.97 mm dan 0.93, 1.34, dan 1.68 mm dalam susunan yang sama. Algoritma rangkaian neural buatan (ANN) menunjukkan kuasa ramalan yang sangat baik apabila dibandingkan dengan MLR. Prestasi kedua-dua algoritma MLR dan ANN berbeza-beza dalam ruang dan musim dengan hasil yang memuaskan adalah di NZ dan kurang memuaskan di SZ. Kedua-duanya menunjukkan data yang lebih baik di kebanyakan bahagian NEM daripada tempoh SWM. Pada umumnya, kedua-dua MLR dan ANN mempamerkan potensi yang besar dalam ramalan TPW di Semenanjung Malaysia dengan yang lebih rendah mengatasi bekas.

**EMPIRICAL MODELS FOR ESTIMATING PRECIPITABLE WATER
USING ADVANCED TIROS OPERATIONAL VERTICAL SOUNDER
SATELLITE DATA OVER PENINSULAR MALAYSIA**

ABSTRACT

Precipitable water (PW) is a highly variable, but important greenhouse gas that regulates the radiation budget of the earth. Adequate knowledge on its distribution, in space and time, is required for a better description and understanding of weather and global climate. The few existing studies in Peninsular Malaysia utilized in situ data to estimate TPW, with the consequences of oversimplifying the situation by masking the effects of local circulation and topographical difference, which are considered important in small scale weather studies. Also, the use of single meteorological parameter to estimate TPW usually undermines other parameters that may have combined effect on the column water vapour. New models based on multiple linear regression (MLR) to estimate TPW have, therefore, been proposed using homogenized climate data records derived from ATOVS onboard NOAA along with surface observations for the period 2001 – 2011. ATOVS data agreed well with radiosonde measurements, both spatially and seasonally, with correlation coefficients (r) ranging from 0.60 – 0.98. New relationship between lower layer (WL) and other layers aloft, of the form $W = \alpha(\varphi)[WL]^{\beta(\varphi)}$ have been proposed, with W being either middle or higher layer PW, α and β are coefficients that are functions of latitude (φ). The models gave r and root mean square error (RMSE) of respective values between 0.867 – 0.926 and 1.65 – 2.38 mm for both the WM and WH predictions across the delineated zones. An overview of the spatial distribution

of seasonal mean TPW showed general decreases from south to north over Peninsular Malaysia, with intense horizontal gradients along the western boundary during the NEM. Spatial and temporal variability of monthly mean of selected meteorological parameters show that annual cycle and spatial pattern of relative humidity are similar to those of TPW, with maximum values obtained in SWM and least during the NEM period. Higher values are spatially found in the SZ with lower values depicted in NZ. Temperature presents almost uniform structures across the zones with maximum values in May/June and least in the month of January. Generally, relative humidity had dominant spatial and temporal impact on TPW in the entire study area. The proposed models gave very encouraging results in all the zones. For the overall period, R^2 was 0.967, 0.946, and 0.935 in NZ, CZ, and SZ respectively, with MBE and RMSE being 0.09, 0.81, -0.97 mm and 0.93, 1.34, 1.68 mm in the same order. Artificial neural networks (ANN) models showed excellent predictive power when contrasted with the MLR models. The performance of both the MLR and ANN models vary in space and season, with best results in NZ and least in SZ. They both showed better data fitting in most part of the NEM than the SWM period. Generally, both the MLR and ANN exhibited great potentials in the prediction of TPW in Peninsular Malaysia with the latter marginally outperforming the former.

CHAPTER 1

INTRODUCTION

1.1 Background of the Study

Atmospheric water vapour, also known as precipitable water vapour or simply, precipitable water (PW), is the gaseous phase of water in the Earth's atmosphere. It is formed due to the constantly changing phases of water within the range of normal atmospheric temperatures because of evaporation, evapotranspiration, vaporisation of liquid water, or the sublimation of ice (Figure 1.1). The amount of water vapour in the air is usually determined through the quantification of its humidity content such as mixing ratio (gkg^{-1}), specific humidity (gkg^{-1}), vapour pressure (hPa or mb), or relative Humidity (%).

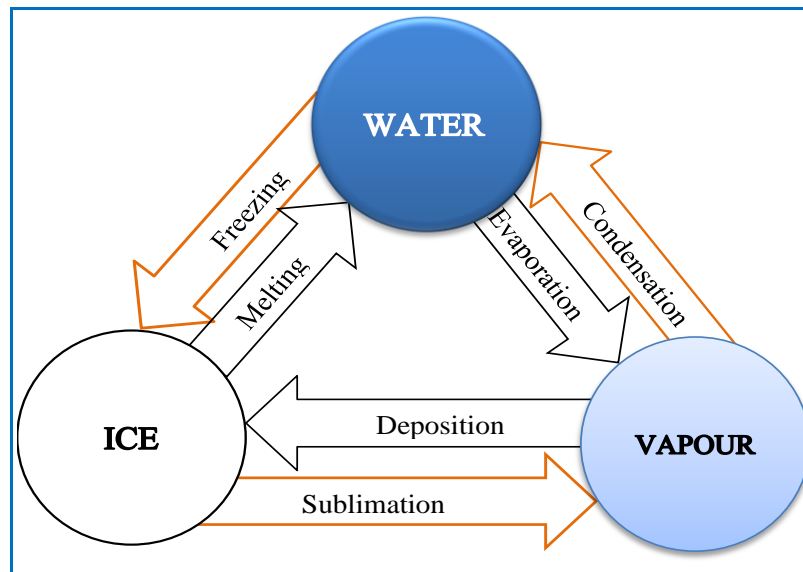


Figure 1.1 Phase transitions of water in the hydrologic cycle

Though PW represents a small percentage (0 – 4%) of the entire atmospheric gas constituents, it is environmentally significant in determining weather and climate

(Lagzi, 2013). Water vapour is arguably the most abundant and most influential of all the major greenhouse gases in the atmosphere. It plays a prominent role in the greenhouse effect (Ernest Raj et al., 2008; Forster and Collins, 2004; Marsden and Valero, 2004) due to its transparency and opacity to shortwave and longwave radiations from the sun and the surface of the earth respectively.

Aside being the most abundant of the greenhouse gases, PW exhibits high spatial and temporal variability, with values ranging from about 50 mm near the equator to less than 5 mm as much at the poles (Mockler, 1995; NCDC, 2013). The global distribution of total precipitable water, whose concentration is indicative at the lower latitudes, is depicted in Figure 1.2. Its spatial variation is more pronounced

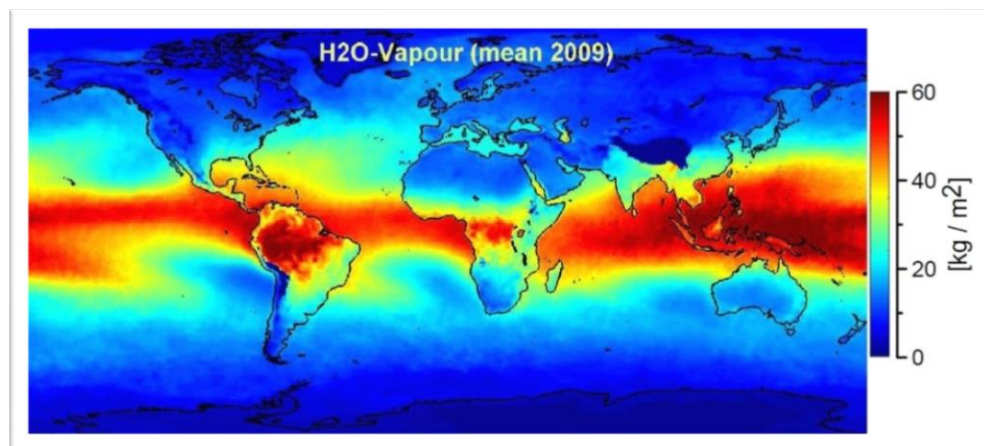


Figure 1.2 Global monthly total precipitable water vapour (TPW) for 2009 derived from Advanced TIROS Operational Vertical Sounder (ATOVS) measurements (Courcoux & Schröder, 2015)

vertically, in which 50% or more is found below the 850 hPa pressure level, while over 90% is confined to the layer below 500 hPa (Peixóto & Oort, 1983). The vertical concentration slides gradually with altitude at higher latitude, but at the lower latitudes it experiences steep vertical decrease (Peixóto & Oort, 1983; Parameswaran & Murthy, 1990) as shown in Figure 1.3. The average residence time

of tropospheric water vapour is about 8 days, with the tropical convergence zones condensing it for about 12 days (Trenberth, 1998) while the residency at subtropical high regions is much shorter (Grody, et al., 2001).

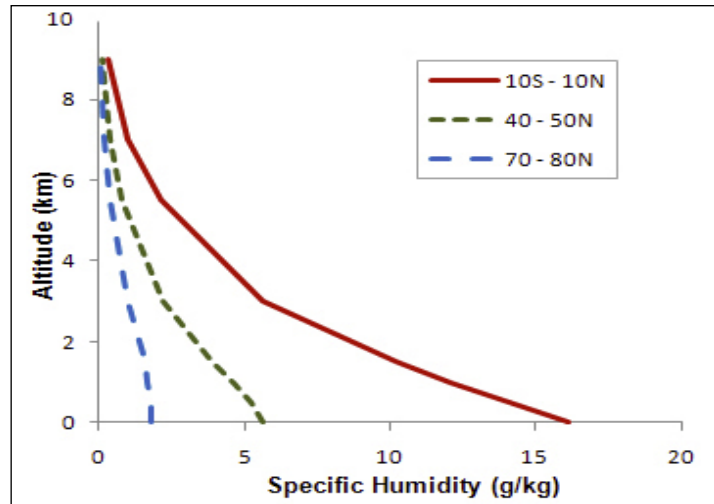


Figure 1.3 Annual mean specific humidity (Oort, 1983). The red solid line indicates humidity variation for the latitude $10^{\circ}\text{S} - 10^{\circ}\text{N}$, the green and blue dash-lines are for latitudes $40^{\circ} - 50^{\circ}\text{N}$ and $70^{\circ} - 80^{\circ}\text{N}$ respectively.

Knowledge of the total vertical column of water vapour is considered more useful than surface humidity, particularly in the studies of radiation budget (Jacob, 2001), and the forecast of precipitation or nocturnal radiation loss, (Tuller, 1977). The determination of horizontal inflow of moisture over an area is useful in the quantitative forecast of the amount of precipitation received by a particular area in a given time or from a given storm (Ojo, 1970). Its role in amplifying global warming, through the provision of the largest positive feedback in model projections of climate change, is acknowledged by Held & Soden (2000). This has led to huge impacts on economic activities such as agriculture, communications, utilities as well as services in a region or local community (Lazo & Demuth, 2009).

Furthermore, a better description and understanding of weather and global climate, requires sufficient knowledge of the distribution and evolution of water vapour, which is a dominant feedback variable in the atmosphere (Dessler & Sherwood, 2009; IPCC, 2007). Its changes in the middle and upper troposphere are particularly crucial in discerning climate change (Held and Soden, 2000). The relevance of PW, particularly, in the tropics includes, but not limited to the provision of: (i) fresh water to drive the economies of most tropical communities through its condensation; (ii) latent heat, during freezing or condensation, for atmospheric motion and convective weather systems, which are important mechanisms for the upward transport of heat in the tropics; (iii) atmospheric correction of high spatial resolution satellite data as well as the enhancement of the precision of land surface temperature estimates.

Peninsular Malaysia, being an equatorial region, is exposed to many climatic factors, including year-round high solar insolation, seasonality in monsoon circulations, the movement of convective systems and higher temperature (Devasthale, et al., 2011). These factors are prominent in the zonal distribution and vertical structure of the climate system. A lot of rain is ushered into the region, particularly during the monsoon seasons, the consequences of which are frequent floods. Monsoon, in the context of this study, connotes a seasonal prevailing wind in South and Southeast Asia regions, blowing as westerlies or easterlies, between May and September and from November to March respectively. In between these periods are inter-monsoon months of April and October.

Due to the foregoing impacts and relevance of PW, there is increasing interest in its measurement at the surface and in its total abundance in a vertical column

through the atmosphere. The latter parameter is called the integrated, columnar, or total precipitable water (TPW), and its estimation is the central subject of this thesis. When measured in linear unit [$1\text{mm} = 1\text{kg}/\text{m}^2$ (IPCC, 2001)], it is defined as the depth (or thickness) of liquid water that collects, if all the vapour in the zenith direction were condensed, at the surface of a unit area (Dupont, et al., 2008; Gruber & Watkins, 1982).

Despite the importance of PW in many different applications, scientists were unable to study its spatial and temporal distribution until global radiosonde data became available in the later part of 1940s (Trenberth, et al., 2005). Figure 1.4 shows the spatial distribution of global radiosonde network as at 2005 and Table 1.1 contains the number of stations that reported to European Centre for Medium-Range Weather Forecasts (ECMWF) in the latter part of 2016.

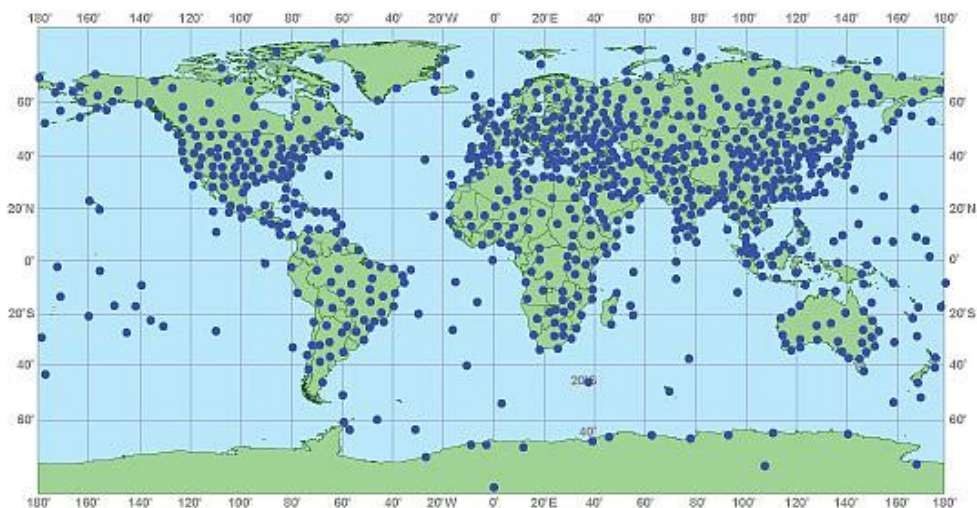


Figure 1.4 Global radiosonde network (Courtesy: NOAA's National Weather Service)

Routine surface meteorological observations, whose global stations distribution is shown in Figure 1.5, are also deployed in the measurements of water

vapour content. Other techniques deployed by the atmospheric science community to estimate PW at the local, regional or global scales include: ground-based microwave radiometers, LIDAR systems, sun photometers or equivalent instruments. Algorithms to derive the PW from temperature measurements by infrared (IR) radiometers as well as satellite observations, have also been deployed. However, each of these methods has its merits and limitations.

Table 1.1 Number of radiosonde stations from which reports are received at ECMWF for 2016 by World Meteorological Organization (WMO) region. For 0000 UTC and 1200 UTC. These are those that report 30 hPa temperature at least 25 times.

Region	Number of Stations	Period of Observations	
		0000 UTC	1200 UTC
Africa	43	25	37
Antarctica	15	9	11
Asia	301	294	265
Europe	155	143	134
North America & Caribbean	156	138	156
South America	55	37	54
Southwest Pacific	97	95	70

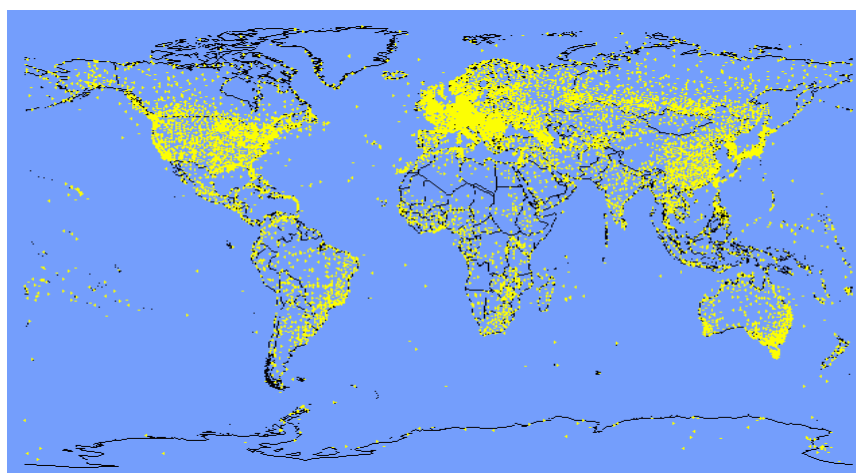


Figure 1.5 Global distribution of integrated surface database (source: NCEI-NOAA).

One of the great challenges of climatological analysis is the issue of inhomogeneous data (Kassomenos & McGregor, 2006), particularly for radiosonde network

(Elliott & Gaffen, 1991). Generally, due to frequent changes in data assimilation systems and models, operational analyses from in situ and satellite observations are short in providing homogenous data sets on the atmospheric moisture budget. In recent decades, however, strong improvements have been witnessed owing to the accuracy of atmospheric model analyses, re-analyses, and forecasts (e.g. Jakobson & Vihma, 2010; Uppala et al., 2005). Retroactively produced (reanalysis) data, based on the utilization of the same model and data assimilation procedure are, therefore, better in this respect.

When the required PW data are scarce or compromised by spatial or temporal homogeneity, the use of empirical models are common practices (Maghrabi & Al Dajani, 2013; Hussain, 1984; Guerova et al., 2005). Such models have been found to be the most popular technique providing both simplicity and straight forward means of estimating the value of PW. Rencher & Schaalje (2008) are also of the view that empirical models in many cases, provide useful approximations of the relationships among variables. Several parametric models of PW, using empirical data, have been developed in the past. The methods are usually based on the statistical fit between the PW data and surface meteorological parameters (e.g. Ruckstuhl, et al., 2007; Maghrabi & Al Dajani 2013).

Very few attempts to parameterize PW over tropical Asia are reported in the literature. For instance, Gautam, et al., (1992) applied a relationship obtained by Liu, (1991) on instantaneous data from the Indian Ocean but got very large root mean square error. Using surface observations for stations in north and central India, Hussain (1984) developed an empirical model for the estimation of PW as a function of air temperature and relative humidity. To the best of the researcher's knowledge,

there is no existing report in the literature, on the use of multiple regression models to parameterized PW in Peninsular Malaysia. The few studies on the quantification of TPW are based on the use of GPS measurements (e.g. Musa et al., 2011; Opaluwa, et al., 2014). Suparta, et al. (2017), however, proposed a method for the estimation of PW in Peninsular Malaysia, applying a one-month surface meteorological data at the Universiti Kebangsaan Malaysia Bangi station, using Adaptive Neuro-fuzzy Inference System (ANFIS) technique. These studies are generally localized point assessment of TPW concentration without enough insight on its behavior or trend elsewhere within the peninsular.

1.1.1 The Structure of the atmosphere

The atmosphere, which consist of 4 major layers: troposphere, stratosphere, mesosphere, and thermosphere, is a blanket of varying air composition that envelops the Earth (see Figure 1.6). Apart from providing gases and regulating heat energy from the sun for the adaptation of life, the Earth's atmosphere plays an important role in the water cycle, just as it shields the Earth from harmful UV rays and small meteors by causing them to be incinerated through friction.

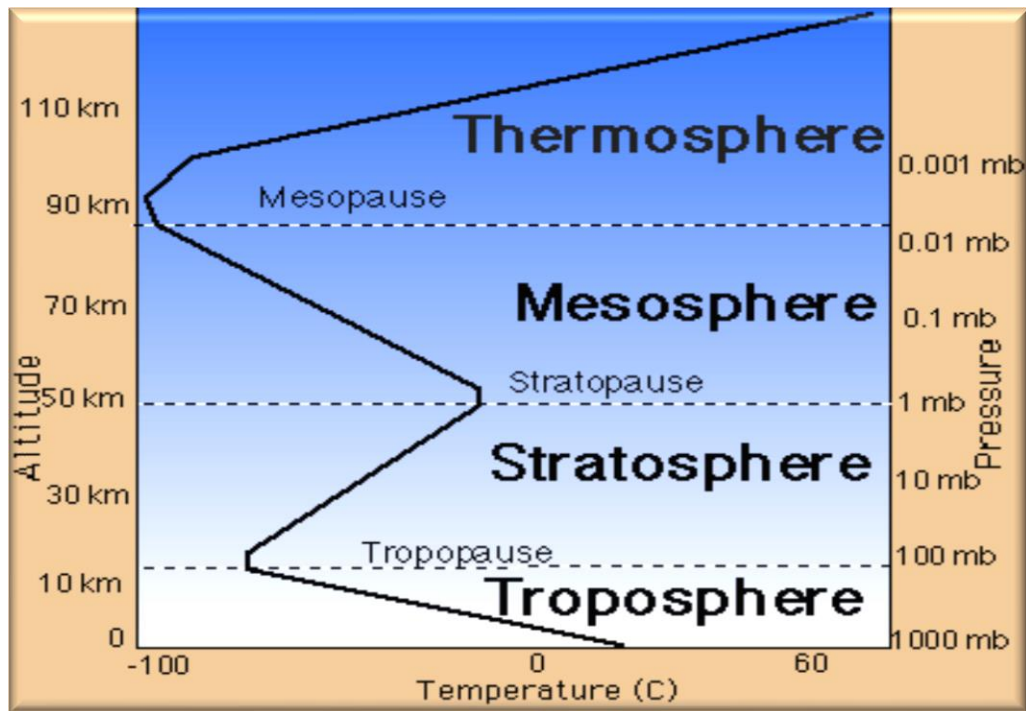


Figure 1.6 The Structure of the Atmosphere, showing the variation of global temperature with altitude and pressure (Teachertech, 2006)

1.1.2 Gaseous composition of the Atmosphere

The Earth's dry atmosphere is composed mainly of nitrogen (N_2), oxygen (O_2), and argon (Ar) (Table 1.2). These gases have limited interactions with the incoming solar radiation and do not interact with the infrared radiation emitted by the Earth. However, there are a number of trace gases, known as greenhouse gases, such as carbon dioxide (CO_2), methane (CH_4), nitrous oxide (N_2O) and ozone (O_3), which absorb and emit infrared radiation. These so-called greenhouse gases, with a total volume mixing ratio in dry air of less than 0.1% by volume, play essential role in the Earth's energy budget. Moreover, the atmosphere contains water vapour (H_2O), which is also a natural greenhouse gas with highly variable volume mixing ratio. Because these greenhouse gases, including H_2O , absorb the infrared radiation emitted by the Earth, they tend to raise its surface temperature.

Table 1.2 Gaseous composition of the atmosphere (Source: <http://geogrify.net/-GEO1/Images/FOPG/03T2>)

Permanent Gases			Variable Gases	
Gas	Symbol	%/Dry Air	Gas	Symbol
Nitrogen	N ₂	78.08	Water vapour	H ₂ O
Oxygen	O ₂	20.95	Carbon dioxide	CO ₂
Argon	Ar	0.93	Methane	CH ₄
Neon	Ne	0.0018	Nitrous oxide	N ₂ O
Helium	He	0.0005	Ozone	O ₃
Hydrogen	H ₂	0.0006		
Xenon	X ₂	0.000009		

1.1.3 Pressure and temperature profiles of the Atmosphere

As shown in Figure 1.6 above, pressure levels in the troposphere and indeed the atmosphere are highest at sea level and decrease exponentially with increase in altitude. Temperature is also higher at low altitudes and generally decreases linearly upwards until the end of the troposphere where there is a discontinuity called the Tropopause. Temperature inversion occur just beyond the Tropopause and then begins to increase further up into the Stratosphere.

1.1.4 The Troposphere

The Troposphere is the lowest of the Earth's atmospheric layers and holds approximately 80 and 99% of its mass and water vapour content respectively. Most of the parameters associated with the temporal evolution of weather are generated in this layer. The average height of the troposphere is ~ 7 km in the Polar Regions and about 20 km at the low latitudes (Danielson et al., 2003). However, these heights have been shown to increase with rising mean temperature. The less convection experienced by air in cold regions compare to warmer areas explains the lower

tropospheric heights at the poles and higher heights at the equator (Geerts & Linacre, 1997).

1.2 Probing the Earth's atmosphere from space

The advent of satellite platforms in geostationary and low-earth orbits has enhanced the observation of earth and its atmosphere, whereby observations are almost simultaneously made at a global scale. This has greatly ameliorated the spatial limitations suffer by ground-based observations, particularly over oceans and remote land areas. Space-based measurements of PW are achieved either from passive microwave sounding or near-infrared (thermal-infrared) channels. Passive microwave observations have the advantage of being able to detect PW on both cloudy and cloud-free atmosphere compared to infrared measurements because they are able to penetrate clouds easily.

NOAA's operational weather satellite system, from which data for the current study are derived, is composed of two types of satellites: geostationary operational environmental satellites (GOES) for short-range warning, and polar-orbiting satellites for longer-term forecasting. The polar orbiters can monitor the entire Earth, tracking atmospheric variables and providing atmospheric data and cloud images. The satellites provide visible and infrared radiometry data that are used for imaging, radiation measurements, and temperature profiles. These satellites send more than 16,000 global measurements daily via NOAA's Command and Data Acquisition (CDA) station to NOAA computers, adding valuable information for forecasting models, especially for remote ocean areas, where conventional data are lacking. Currently, NOAA is operating five polar orbiters. The newest being NOAA-19,

which was launched in 2009. NOAA-15 to -18, however, continue to transmit data as stand-by satellites.

The Advanced [Television Infrared Observation Satellite (TIROS) Operational Vertical Sounder (ATOVS)] suite of instruments; High Resolution Infrared Radiation Sounder (HIRS); Advanced Microwave Sounding Unit-A and -B (AMSU-A/B); and Microwave Humidity Sounder (MHS), on NOAA and Meteorological Operational (Metop) satellites, represent infrared spectrometers and microwave radiometers. The combination of these three instruments contains enough information to infer atmospheric profiles of temperature and specific humidity. Satellite Facility for Climate Monitoring (CM-SAF) provides water vapour products, retrieved from ATOVS, with comparably high spatial resolution at the regional and global scales,

1.3 Statement of the Research Problem

The variability of PW in space and time, including its radiative features, poses a great challenge in its sampling and measurement. This explains why several different techniques are used by scientists to quantify the parameter. The traditional profiling instruments, such as Radiosonde, GPS, and Water Vapour Radiometer (WVR), have varying limitations as mentioned in subchapter 1.1 above. For instance, the accurate instantaneous data obtained from radiosonde system (Nash et al. 2011) is thwarted by its temporal and spatial heterogeneity (Oltmans & Hofmann, 1995), particularly in Peninsular Malaysia, where only four stations are currently operational. Although GPS are adjudged to perform well under clear and rainy/cloudy weather (Solheim, et al., 1999), the ground-based receivers, especially in the tropics, are spatially sparse (Musa et al., 2011; Opaluwa, et al., 2014). For

instance, Musa et al. (2011), have identified very few Continuously Operating Reference Stations (CORS) for effective calibration of the GPS profiles. Water Vapour Radiometer (WVR), in addition to being limited in spatial resolution (Lanzante, et al., 2003), its performance deteriorates under intense convective weather (Chan, 2009).

By contrast, since the tropics have a relatively homogeneous air mass and fairly uniform distribution of surface temperature and pressure than the mid- and higher- latitudes, local and mesoscale systems are considered more important in weather studies than synoptic system (Gaffen, et al., 1992; Trenberth et al., 2005). The limitations of the traditional profiling instruments in the peninsular, however, makes the studies of spatial and temporal variability of PW and its prediction, over large area, unreliable. This is because large areas of great local diversity have generally been treated as unity by previous quantifiers. The oversimplification of the situation by these macro-studies can be seriously misleading since the effects of small topographical differences and local circulation are most likely to be eclipsed.

The few investigations on the estimation of PW in Peninsular Malaysia, cited earlier, were also unmindful of the variability in the vertical profile of humidity, which plays significant roles in the accurate estimation (or prediction) of precipitable water (e.g. Tuller, 1977; Gaffen, et al., 1992). Furthermore, the use of single meteorological parameter (e.g. mixing ratio, specific humidity, etc.), which may be compromised by either measurement accuracy, data coverage, or analysis uncertainty, by most scholars to empirically estimate PW, undermines other parameters (e.g. surface pressure, station height, temperature, etc.) that have combined effect on the TPW above an area.

To ameliorate the limitations posed by the various tools deployed in estimating PW, i.e. the use of few meteorological parameters, and limited knowledge on its vertical component, particularly in Peninsular Malaysia, multiple linear regression (MLR) models become imperative. Homogenized humidity data from ATOVS are, therefore, used to propose empirical relationships between: (i) the surface and other isobaric layers of PW. (ii) TPW and selected surface meteorological parameters (temperature, pressure, and relative humidity) for Peninsular Malaysia.

1.4 Aim and Objectives

The aim of the research is to develop models, based on surface meteorological parameters, for the estimation of TPW in Peninsular Malaysia, with the following specific objectives:

- i. To analyse the behaviour of TPW and layered precipitable water (LPW) over Peninsular Malaysia, using data retrieved from radiosonde and ATOVS on board NOAA and Meteop satellites, as an initial step in establishing data climatology in the study area.
- ii. To evaluate the spatial distributions and temporal variations of PW from ATOVS as well as establishing empirical relationships between the boundary layer and upper layers of the humidity quantity.
- iii. To determine the impacts of temperature, relative humidity, and pressure on TPW over the study area.
- iv. To develop models using multiple linear regression (MLR) method and comparing with artificial neural network (ANN) models for the

prediction of TPW in Peninsular Malaysia, using surface temperature, relative humidity, and pressure as input parameters.

1.5 Research Question

Previous empirical methods to estimate TPW have been deployed by many researchers at different stations and regions as reported in subchapter 1.1. Some salient questions, therefore, arise in the quest to establish models to predict PW in Peninsular Malaysia. These include: (i) to what extent does the ATOVS-retrieved data agree, both in space and time with the radiosonde-derived data over Peninsular Malaysia? (ii) how is PW distributed both in space and time over Peninsular Malaysia? (iii) is there any empirical relationship between the lower layer PW and other layers aloft? (iv) how does TPW relate with surface meteorological parameters (temperature, pressure, and relative humidity)? (v) can the relationship in (iv), if any, be determined using multiple linear regression models? (vi) given values of the screen level parameters, can the determined relationship effectively predict TPW? (vii) how accurate can the method of Artificial Neural Networks (ANN) predict TPW compared to the MLR method?

1.6 Research Hypothesis

Generally, it is believed that effective relationship between PW at the boundary (surface) layer in the troposphere with other layers aloft, points to possible relationship between TPW and surface moisture content (e.g. specific humidity, mixing ratio, dew point, vapour pressure, or relative humidity).

Columnar relative humidity, for a given site in tropical climate, assumes a C-shape structure with values gradually decreasing with rising altitude, culminating at

least values in the mid-troposphere. Higher up towards the upper troposphere, the trend resumes increasing tendency with height up to the tropopause (Folkins, et al., 2002). This, points to a possible linear relationship between RH and PW, which is also noted to decrease with altitude. It is therefore, expected that higher PW implies higher RH and vice versa. Decreasing temperature and pressure with altitude within the troposphere, as seen in subchapter 1.1.1, also indicate some form of relationships between the duo and TPW.

From the foregoing, the method of MLR model can be used to build a relationship between TPW and the three parameters (temperature, pressure, and relative humidity). Considering the carefully reanalysed ATOVS data over a region, it is possible to develop predictive models that combine satellite and surface data for the accurate prediction of TPW, with temperature, relative humidity and pressure factored in as input variables. The predicted TPW is expected to compare very well with that derived from the radiosonde technique, which is regarded as the standard water vapour profiling instrument.

1.7 Scope of the Study

This research is limited to establishing the variability of precipitable water, and developing models, based on MLR, to quantify TPW using homogenized ATOVS data and the meteorological variables mentioned in section 1.4. The period covered by the study is between 2001 and 2011, with the geographical scope being Peninsular Malaysia, as described in subchapter 3.2. Peninsular Malaysia was selected for this study because of the high amount of atmospheric water vapour experienced, mainly due to the high evaporation rates ascribed to the prevailing monsoons that exhibit seasonal changes within the region. Though the homogenized

ATOVS data are available from 1999 to 2011, the first 2 years are constraint in quality due to a large number of missing values, which explains the use of only 11 years observations.

Empirical relationships between the isobaric layers of tropospheric water vapour, using ANOVA technique on ATOVS data, have also been developed in the study. Although climate models, based on computer simulations, have become widely used tools for the study of global and regional climate phenomena, the approach has not been used in the current study. This research has been restricted to the use of actual satellite-retrieved, radiosonde-derived (for validation) data, and surface observations from selected meteorological stations across Peninsular Malaysia (see Figure 3.1). ANN models, with TPW as output and the selected meteorological variables as inputs have also been developed and compared with the proposed MLR models. An attempt has also been made to explore the spatial distribution and seasonal variations of tropospheric water vapor over the peninsular.

1.8 Novelty and Significance of the Study

Knowledge of the spatial distribution and temporal variability of PW, both in the vertical and horizontal dimensions, is not only important in forecasting regional weather and the understanding of the global climate system, but also for information on weather variability, as mentioned earlier. Therefore, for precise prediction and modelling of weather, the required information on the vertical profile of its parameters needs accurate and continuous gathering, both in time and space (Shuman, 1978). Due to the spatial limitations of the various water vapour profiling instruments and platforms, particularly in the current study area as earlier enumerated, an attempt has been made to mitigate the over masking of local

circulations occasioned by the scarcity of homogenous spatial and temporal data. This is achieved by using retroactively homogenized data from ATOVS to develop empirical models for the estimation of both LPW and TPW for Peninsular Malaysia.

This study, based on available literature, is the first to develop and apply empirical methods for the estimation of both layered and total precipitable water over the entire Peninsular Malaysia using satellite and surface observations across data void regions. It is also the first to formulate inter-layer PW relationship with latitude factored in. Moreover, novel MLR models, from the amalgamation of satellite and surface observations, for the estimation of TPW in the study area have been developed. The use of ANN model to produce models capable of estimating TPW using satellite data in the study area also appears to be unique. The first ATOVS data climatology, involving a distinctive picture of both temporal and spatial variability of layered and total precipitable water over Peninsular Malaysia, has been conducted.

The proposed models, apart from being cost effective, are expected to provide simple means for continuous estimation of TPW as an initial input in local weather predictions for environmental and meteorological applications. More so, the analysis of the temporal and spatial variability of PW, spanning a period of 11 years, is expected to provide further understanding on its distribution patterns, which is vital in the effective mitigation of weather and climate impacts in the study area, as already stated.

1.9 Thesis Outline

The content of this dissertation, which is structured into five broad sections, organized as chapters, is briefly outlined in the following paragraphs;

Chapter 1 is on the general introduction of the entire research, and commences with the background of the study, providing an overview of the thesis. This is immediately followed by a brief description of the vertical structure of the atmosphere, with its gaseous composition as well as the profiles of pressure and temperature. The roles and significance of PW measurements in the climate system are also outlined in this chapter. The research problem and objectives, as well as the research question and hypothesis, are all presented here. The chapter concludes with a highlight of scope, novelty and significance of the study.

A broad review of relevant and related literature in previous studies on precipitable water is presented in Chapter 2. The essence is to locate the knowledge gaps that require filling in the current research. The review is carried out in different segments. First, the importance of PW study is identified. Secondly, brief description of global and regional wind patterns, and also some impacts of precipitable water in the tropics are reviewed to reveal the significance of the study. Thirdly space-based and in situ observations of TPW are reviewed to establish data climatology. Fourthly, various techniques used for the global, regional and meso-scale estimation of precipitable water, as documented by previous scholars, have been reported. Finally, a brief review of temporal and spatial variability of precipitable water studies at the global, regional and local levels is done.

Chapter 3 hosts the description of the geographic and climatic representation of the study area. The description of the data sets and their sources as well as the software and tools used are presented in this chapter. Details of data pre-processing steps and techniques/methodology used to achieve the desired objectives are contained in the chapter as well.

In Chapter 4, results of findings are analysed and discussed, including comparison between ATOVS-retrieved and radiosonde-derived data. The results of the vertical distribution of PW and the formulation of inter-layer relationship are presented and discussed. The impacts of the selected meteorological variables on TPW are analyzed and the results of the MLR models are compared with those obtained using ANN models.

Chapter 5, which is the concluding chapter, presents summary of the results and suggestions for future research.

CHAPTER 2

LITERATURE REVIEW

2.1 Introduction

With the principal desire of this dissertation being the utilization of data from satellite and surface observations to develop models for estimating precipitable water over a region, relevant studies in literatures are reviewed in this chapter. The review includes the role of precipitable water in the atmosphere and the relevance of its quantification. Various platforms and techniques used in the quantification of precipitable water in literatures have been surveyed to identify knowledge gaps in order to address same in this study. Some previous studies on global and regional climatology of TPW particularly, in the tropics have also been reviewed. cursory looks at some empirical formulation of layered and total precipitable water, particularly, on linear regression and artificial neural networks techniques, have also been delved into in the chapter.

2.2 Importance of Precipitable Water Study

Measurement of precipitable water in the atmosphere is particularly important. Being the most important natural greenhouse gas, PW exerts great influence on the radiation budget of the Earth's atmosphere and, thus, affects our climate. Additionally, water is also responsible for the formation of clouds and precipitation, which makes its quantification an essential measurand in all climate models. However, when weather forecasting and climate development are desired, accurate estimation of atmospheric water vapour is imperative (Möhler et al., 2008). Knowledge of the amount of water present in the atmosphere, both horizontally and vertically, is vital in many applications, including the hydrologic cycle (Schneider, et

al., 2010), radiation balance (Jacob, 2001; Courcoux & Schröder, 2015), and the predictions of cloud and precipitation (Tuller, 1977; Sherwood, et al., 2010; Wang, et al., 2010).

2.2.1 The hydrologic cycle

The hydrologic cycle describes the movement of water, within and between the Earth's atmosphere, continents, and oceans, in its three phases. The vapour form, also called precipitable water vapour, plays a cardinal role in the hydrologic cycle, in which the climate and weather systems are affected (Follette, et al., 2009). This cycle begins with evaporation of water from the surface of oceans when moist air in form of water vapour, is lifted due to temperature difference between the surface and the atmosphere, cools and condenses to form clouds. The moisture is then transported around the globe until it finally returns to the surface as precipitation.

Once at the surface of the earth, some of the water may percolate and become groundwater while some eventually evaporate back into the atmosphere. The groundwater is either released into the atmosphere through transpiration or seeps itself into streams, rivers, lakes or oceans. The remaining water on the surface of the Earth, known as runoff, is then emptied into either lakes, rivers or streams and transported back into the oceans to recommence the cycle. The vapor phase redistributes energy occasioned by evaporation and condensation due to its fast movement in the atmosphere. This movement is strongly linked to precipitation and soil moisture, which have important practical implications (AGU, 1995). Figure 2.1 is a schematic representation of the hydrologic cycle showing estimates of the current global water budget and its annual flow using observations from 1979 – 2000 (Trenberth, et al., 2007).

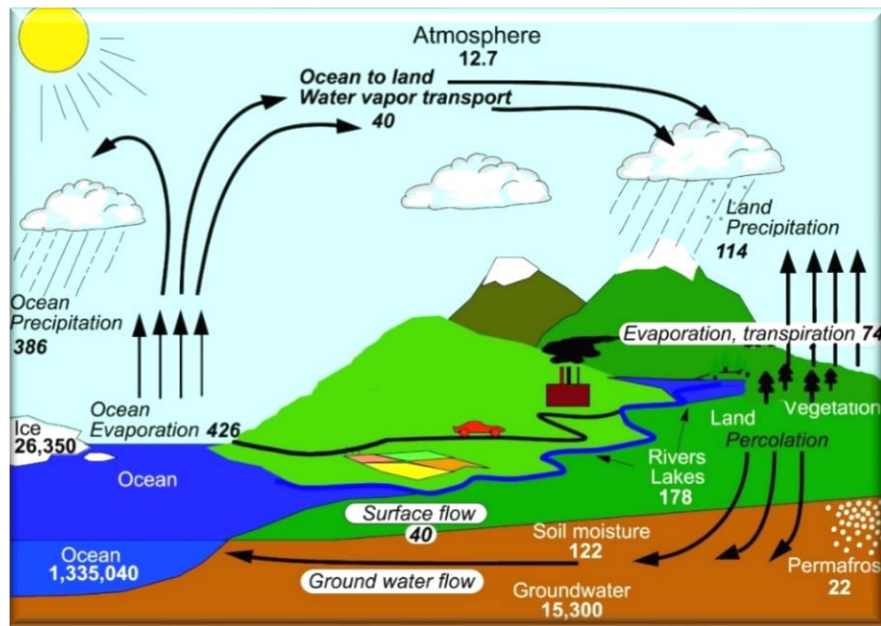


Figure 2.1 Long-term mean estimates of global water budget and its annual flow based on Trenberth, et al. (2007). Estimates are in 10^3 km^3 for storage and $10^3 \text{ km}^3/\text{year}$ for exchanges.

2.2.2 The effects of precipitable water on radiation balance

Being respectively transparent and opaque to solar and terrestrial radiations, precipitable water acts as a greenhouse gas (Forster & Collins, 2004; Marsden & Valero, 2004; Ernest Raj et al., 2008). The climate of the Earth, therefore, supports life in large part due to the greenhouse effect in collaboration with the workings of the hydrologic cycle. For instance, water vapor is involved in an important climate feedback loop that exerts great influence on the radiation budget of the Earth's atmosphere which affects our climate. This is seen in the increase of atmospheric temperature in response to increasing Earth's surface temperature, causing the atmosphere to hold more water vapor. As a greenhouse gas, therefore, water vapor absorbs energy that would otherwise escape to space, thereby causing further warming. The water vapour greenhouse feedback is viewed as the strongest positive feedback in the climate system (e.g. DelGenio, et al. 1991). Observational studies by

Duvel & Breon (1991), who relied on correlations between satellite measurements of column water vapour over open oceans and sea surface temperature, have also lend credence to the positive feedback of the greenhouse effect.

Water vapour is also crucial to the energy balance processes within the climate system by modulating and transmitting radiative energy between space and the Earth's surface, through the atmosphere (Held and Soden 2000), as well as in the transfer of latent heat from the surface to the atmosphere (Trenberth, et al., 2011). The laws of thermodynamics constrain the humidity structure of the atmosphere as water transits through vapour and condensate (Stevens & Bony, 2013). For instance, it is common for water, which is a phase-changing substance, to have maximum saturated (or partial) pressure as a strongly increasing function of temperature that is governed by the Clausius-Clapeyron relation. A physical relationship exists in the Clausius-Clapeyron relation which provides that for liquid water to transit to vapour phase, energy at constant pressure is required. This is such that whenever vapour pressure exceeds the saturation vapour pressure, a condensation linked to latent heat released occurs. According to Allan (2012), the Clausius-Clapeyron equation, which poses a fundamental controls on the climate system, provides a powerful constraint on how saturated moisture content varies with air temperature. This constraint places only an upper bound on the dependent of water content on any temperature. However, its implications for weather and climate is not straightforward because water vapour is mostly unsaturated in the atmosphere (Pierrehumbert & Roca, 2007). Nevertheless, the dynamical effects of radiation and convection provide foundation for discerning wide characteristics of the circulation of the atmosphere, especially in the tropics, where water is often saturated (Stevens & Bony, 2013).

2.2.3 Predictions of clouds and precipitation

TPW is regarded as a necessary condition for rainfall. Areas of relatively high precipitable water, also known as atmospheric rivers or moisture plumes, are often associated with intensive rainfall events (Junker et al., 2008). It is, therefore, expected that increased atmospheric moisture automatically results to increased precipitation. This relationship is, however, not straight forward because several factors, including convection, horizontal flow dynamics, and the presence of cloud condensation nuclei, contribute to the occurrence of rain. Nonetheless this humidity variable can be used as surrogate for the forecast of cloud and precipitation (Sherwood et al., 2010).

The interaction between TPW and precipitation is such that within the horizontal large-scale advection, the small-scale motions often interact with the water vapour field through a convective process. This process occurs mainly when an air parcel rises by itself in an unstable atmosphere. During airlift, the parcel expands and cools at the dry adiabatic temperature lapse rate of $9.8\text{ }^{\circ}\text{C}/\text{km}$ (Stevens & Bony, 2013), causing its saturation vapour pressure to decrease. The parcel then continues its updraft, so long as its adiabatic lapse rate is less than the lapse rate of the surrounding atmosphere, until dew point temperature is reached and subsequent condensation (cloud formation) occurs. As long as the air parcel is warmer than its surrounding, the upward movement will continue unabated, resulting in continuous condensation of water vapour. Consequently, a steady release of latent energy then reduces the adiabatic cooling of the parcel. This indicates the generous contribution of moist convection to the vertical transport of heat and moisture on various scales (Pierrehumbert et al., 2007). Weather and climate are, therefore, influenced by water